Calculation of anomalous magnetic moments of strange baryons

B. B. Deo and L. P. Singh
Physics Department, Utkal University, Bhubaneswar-751004, Orissa, India
(Received 4 December 1974)

Sidewise dispersion relations are used to calculate the anomalous magnetic moments of strange baryons. The absorptive parts of the relevant form factors are related to the real parts of the photoproduction amplitudes. Assuming that the absorptive part is given correctly by the lowest intermediate meson-baryon state, the low-lying resonances below inelastic threshold, and a high-energy fall-off calculated by Reggeizing the photoproduction amplitude, we obtain the imaginary parts for all energies by extrapolation using a suitable conformally mapped variable. Values for the anomalous magnetic moments are obtained which are significantly different from the SU(3) predictions. In nuclear magnetons, the results are $\kappa_\Lambda = -0.545$, $\kappa_{\Sigma^0} = 0.4$, $\kappa_{\Sigma\Lambda} = 0.97$, $\kappa_{\Sigma^-} = -0.493$, $\kappa_{\Sigma^+} = 1.293$, $\kappa_{\Xi^-} = -0.297$, $\kappa_{\Xi^0} = -0.214$, in fair agreement with recent experimental values for these moments.

I. INTRODUCTION

Experimental values for the magnetic moments of the strange baryons Λ, Σ, and Ξ have been reported recently.[1] Even though the results are not very accurate for the Σ and Ξ particles, the values of the moments are many standard deviations away from the SU(3) predictions. In SU(3) one predicts the magnetic moments of these strange baryons from the more accurately known magnetic moments of the neutron and the proton.[2] Therefore, theoretical attempts had centered heavily on explaining the anomalous values of the nucleons. Since recent experimental values differ appreciably from the SU(3) predictions, theoretical models have to be reexamined.

The anomalous parts of the magnetic moments are assumed to be due to the strong-interaction corrections to the baryon electromagnetic current. Since Feynman-Dyson-type perturbation theory fails in the case of strong interactions, perturbation calculations always yield values which are quite different from experimental values. In one of the earliest perturbation calculations of anomalous magnetic moments of baryons Katsumori,[3] faced with the lack of knowledge of various baryon-baryon-meson coupling constants, took all the coupling strengths to be unity. He considered contributions of all possible baryon-meson intermediate states. The values of magnetic moments one gets from his equations after correcting his results by using SU(3) coupling strengths with $D/(D+F) = 0.67$ are shown in Table I. These values differ widely from the experimental one. Drell and Pagels[4] were the first to use sidewise dispersion relations and to point out that the low-energy states contribute predominantly to the static magnetic moments of the nucleons. They also correctly stressed the importance of incorporating the exact threshold behavior of the relevant amplitudes. However, they were constrained to use a high-energy cutoff. Continuing their ideas, Pagels[5] calculated anomalous magnetic moments of all the baryons. He was able to reproduce the SU(3) relations by including only the contributions of charged meson states to the absorptive amplitudes. In the limit of degenerate baryon masses and vanishing meson masses his results, even for nucleon anomalous moments, differed from the experimental values. This difference was attributed to the assumed mass degeneracy. But calculation with physical baryon and meson masses using SU(3)-symmetric coupling constants with $F/D = 0.6$ led to deviations from SU(3) predictions and in most cases from the experimental results as well (see Table I). The major contribution to symmetry breaking came from the nondegeneracy of the thresholds of the competing processes. The reasons for deviations from experiment were, however, thought to be twofold. Firstly, the pole terms need not approximate the exact amplitude away from the threshold. Secondly, a realistic calculation should include effects of symmetry breaking on the baryon-meson coupling constants. The inclusion of rescattering terms by Pagels is the main source of the difference between his and Katsumori's perturbation results. In a recent calculation of anomalous magnetic moments of nucleons[6] based on sidewise dispersion relations[7] and the concepts of analytic approximation and extrapolation,[8] we supplemented the idea of the exact threshold behavior with a possible Regge falloff at high energies. The Regge decrease made the dispersion integral finite. The Regge falloff is calculable since the absorptive part is related to the photoproduction amplitude. The conformal mapping technique was utilized to incorporate the exact threshold behavior and the Regge high-energy constraints into the absorptive amplitudes. The absorptive amplitudes for all

energies were obtained as extrapolations of the contributions from the lowest-mass intermediate state (the one-pion–one-nucleon state) and the low-lying resonances to the related photoproduction amplitudes up to the inelastic threshold. The results were in excellent agreement with the experimental values. The present work is an extension of our model of calculating anomalous magnetic moments to the cases of the strange baryons.

In Sec. VI we discuss the salient features of our calculation for the strange baryons and the reasons our results differ significantly from the SU(3) values. In Sec. II we indicate the extrapolation procedure for the absorptive amplitudes. Section III contains calculations of Λ, Σ^0, and $\Sigma\Lambda$ moments. In Sec. IV we report the results of calculations of $\Sigma^{\pm}$ magnetic moments, and calculations of $\Xi^{-,0}$ magnetic moments are given in Sec. V.

II. EXTRAPOLATION PROCEDURE FOR ABSORPTIVE AMPLITUDES

The general form of the electromagnetic vertex of a baryon with the incoming baryon and the photon on their mass shells and the outgoing baryon off its mass shell (see Fig. 1) consistent with Lorentz invariance, parity, time reversal, and the generalized Ward identity is

$$\begin{aligned} e\Gamma_\mu u(p_1) = e\{&\gamma_\mu + [(-i\sigma_{\mu\nu}k_\nu/2m_1)F_2(W^2) + k_\mu F_3(W^2)] \\ &\times[(m_1 + \not{p}_1 + \not{k})/2m_1] \\ &+ [(-i\sigma_{\mu\nu}k_\nu/2m_1)F_2(W^2) + k_\mu F_3(W^2)] \\ &\times[(m_1 - \not{p}_1 - \not{k})/2m_1]\}u(p_1). \end{aligned} \tag{1}$$

$F_2(W^2)$ is easily recognized as yielding the value of the anomalous magnetic moment in the limit $W^2 = m_1^2$. The form factor $F_2(W^2)$, as a function of W^2, is analytic in the entire complex W^2 plane with a cut extending from W_{th}^2 to ∞, where $W_{\text{th}}^2 = (m_2 + m_\mu)^2$, the threshold for the lightest intermediate two-particle state contributing to the absorptive amplitude. Assuming $F_2(W^2) \to 0$ as $W^2 \to \infty$, we take the dispersion relation for $F_2(W^2)$ to be an unsubtracted one,

$$F_2(W^2) = \frac{1}{\pi}\int_{W_{\text{th}}^2}^{\infty} \frac{\text{Im}F_2(W'^2)dW'^2}{W'^2 - W^2}. \tag{2}$$

Note that $\kappa = F_2(m_1^2)$ is the anomalous magnetic moment. Below the inelastic threshold we assume the absorptive amplitudes are given exactly in terms of the Chew-Goldberger-Low-Nambu[9] (CGLN) invariant photoproduction amplitude A,

$$\begin{aligned} \text{Im}F_2(W^2) = &\frac{m_1 g|q|}{8\pi W m_N(W^2 - m_1^2)} \\ &\times \int_{-1}^{+1} d(\cos\theta)(m_2 p_1 \cdot k - m_1 p_2 \cdot k)\text{Re}A, \end{aligned} \tag{3}$$

where m_1, p_1 and m_2, p_2 are masses and four-momenta of the incoming and intermediate baryons, respectively, m_N is the nucleon mass, and W and q are the center-of-mass energy and meson momentum as shown in Fig. 2. g is the baryon-baryon-meson coupling strength and θ is the scattering angle.

Using the pole terms of the meson photoproduction amplitudes, we find that in the limit $m_\mu/m_2 \to 0$ the absorptive parts behave as

$$\text{Im}F_2(W^2) = \frac{g^2}{4\pi}\frac{W^2 - m_2^2}{4m_2^2} \cdots . \tag{4}$$

In the specified limit this corresponds to the exact amplitudes at threshold by the Kroll-Ruderman theorem.[10]

To obtain the high-energy contribution the photoproduction amplitudes are Reggeized by the replacements[11]

$$\frac{1}{t - M^2} \to \frac{d\alpha}{dt}\frac{\pi}{\sin\pi(\alpha - J)}\frac{1 + \tau e^{-i\pi\alpha}}{2}s^{\alpha(t)-J}, \tag{5a}$$

$$\frac{1}{u - M^2} \to \frac{d\alpha}{du}\frac{\pi}{\sin\pi(\alpha - J)}\frac{1 + \tau e^{-i\pi\alpha}}{2}s^{\alpha(u)-J} \tag{5b}$$

for meson and baryon pole terms, respectively. $\alpha = J$ at the pole t or $u = M^2$ and τ is the signature

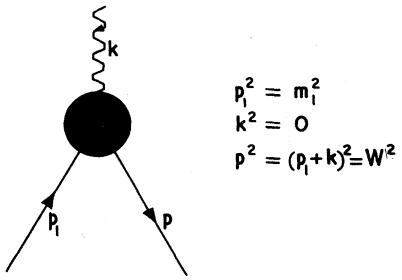

FIG. 1. Fermion-photon vertex.

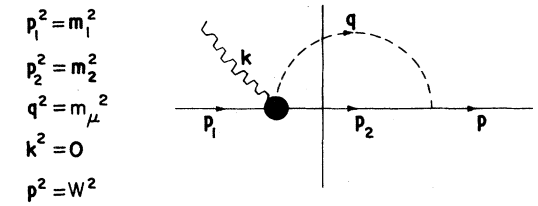

FIG. 2. Pseudoscalar-meson–baryon intermediate-state contribution to the absorptive part.

factor. An absorption factor e^{bt} with $b \simeq 1.5$ (see Ref. 12) was inserted for the t-channel pole terms to account for a rapid falloff of photoproduction amplitudes at forward angles. Equation (3) was then integrated with these replacements and a graph of absorptive parts against $\ln(W^2)$ was plotted. The absorptive amplitudes were found to vanish as $(W^2)^{-\nu}$ for large W^2. The values of ν were determined separately for each of the baryons.

Armed with the threshold behavior from perturbation theory and the high-energy behavior from Regge theory, one can extrapolate to the inelastic region most effectively by mapping the cut plane of analyticity onto the interior of a circle of unit radius. The mapping is

$$Y = \frac{W^2 - W_0^2}{[(W^2 - W_{\rm th}^2)(W^2 - W_{\rm in}^2)]^{1/2} + [(W_0^2 - W_{\rm th}^2)(W_0^2 - W_{\rm in}^2)]^{1/2}}, \tag{6a}$$

$$Z = \frac{1}{Y}[1 - (1 - Y^2)^{1/2}], \tag{6b}$$

with $W_0^2 = W_{\rm th}^2 - 4m_2^3/m_\mu$, so that Im $Z \sim (W^2 - m_2^2)$ at threshold $W^2 = W_{\rm th}^2$ in the limit $m_\mu/m_2 \to 0$. The sketch of the mapped plane is shown in Ref. (6). We then write

$$F_2(W^2) = \Psi_R(Z) \sum_n a_n \phi_n(Z), \tag{7}$$

where the $\phi_n(Z)$'s are a set of orthonormal polynomials in Z given by

$$\phi_n(Z) = \sum_{m=0}^{n} b_m^n Z^m \tag{8}$$

and satisfy

$$\int_\Gamma \phi_m^*(Z)\phi_n(Z)dZ = \delta_{mn} \tag{9}$$

where Γ is the elastic contour. The Regge factor $\Psi_R(Z)$ is given by

$$\Psi_R(Z) = \left(\frac{1 - Z}{1 - Z^*}\right)^\beta [(1 - Z)(1 - Z^*)]^\gamma. \tag{10}$$

For a given n the coefficients a_n are calculated by inverting an $n \times n$ matrix, obtained by equating Im $F_2(W^2)$ of Eq. (7) at n equally spaced W^2 points in the elastic region with perturbation values of Im $F_2(W^2)$ as given by Eq. (3) with A consisting of Born and low-lying resonance terms. High-energy phase factors β are obtained by doing a best-fit calculation over the entire elastic region.

The absorptive amplitudes as given by Eq. (7) are now assumed to extrapolate correctly into the inelastic region. This method is now applied to individual baryons as detailed below.

III. ANOMALOUS MAGNETIC MOMENTS OF Λ, Σ^0 AND $\Sigma\Lambda$ TRANSITION MOMENT

Consideration of the interaction of photons with charged particles selects out NK and ΞK as the only two possible intermediate states which make contributions to the anomalous magnetic moments of Λ and Σ^0 and the transition moment of Σ^0 to Λ. However, the threshold for the ΞK state lies much higher than that for the NK state. In fact ΞK opens only after the inelastic threshold in the NK channel, namely, the threshold for $NK\pi$ production. One of our important observations in our previous work (Ref. 6) was that soon after the inelastic threshold, the multiparticle production effects strongly damp the amplitude. Hence the contribution of the ΞK state to the absorptive amplitude can be omitted. It may be noted that $\Sigma\pi$ is allowed by various quantum-number conservation principles. But contributions to the absorptive part due to states $\Sigma^+\pi^-$ and $\Sigma^-\pi^+$ sum up to zero. So the contributions from the NK channel to the absorptive amplitude will be the dominating two-body intermediate-state contribution below inelastic threshold.

TABLE I. Comparison of the experimental values (in nuclear magnetons) of the anomalous magnetic moments of strange baryons with the calculated values (perturbation-theory calculation, Pagels's results, and the present authors' results).

Anomalous magnetic moments of strange baryons	Katsumori's results with SU(3) coupling strength	Pagels's results I [SU(3) predictions]	Pagels's results II	Present calculation	Experimental values
κ_Λ	−1.185	$\frac{1}{2}\kappa_n$	−0.66	−0.545	-0.67 ± 0.06
κ_{Σ^+}	0.952	κ_p	1.2	1.293	1.59 ± 0.45
κ_{Σ^-}	0.880	$-(\kappa_p + \kappa_n)$	−0.7	−0.493	-0.48 ± 0.37
κ_{Σ^0}	0.916	$-\frac{1}{2}\kappa_n$	0.2	0.4	···
κ_{Ξ^-}	1.073	$-(\kappa_p + \kappa_n)$	−0.1	−0.297	-0.9 ± 0.75
κ_{Ξ^0}	−1.990	κ_n	−0.8	−0.214	···

For the photoproduction processes $\gamma+\Lambda\to p+K^-$ and $\gamma+\Sigma^0\to p+K^-$ the s channel is closed and A is given by the u-channel processes $\gamma+p\to\Lambda+K^+$ and $\gamma+p\to\Sigma^0+K^+$. Use of these Born terms in Eq. (3) reproduces the perturbation-theory result. Inclusion of low-lying resonances such as K^* in the t-channel and $N^*(1460)$ in the U channel for Λ and $N^*(1460)$ and $\Delta(1236)$ for Σ^0 and $\Sigma\Lambda$ modifies the amplitudes to

$$A_\Lambda=\frac{eg_{\Lambda pK}}{u-m_2^{\,2}}+\frac{g_{\gamma KK^*}g^{E}_{K^*\Lambda p}(m_1+m_2)}{m(t-m_{K^*}^{\,2})}+\frac{g_{\gamma KK^*}g^{M}_{K^*\Lambda p}t}{m(m_1+m_2)(t-m_{K^*}^{\,2})}+\frac{g_{\gamma pN^*}g_{N^*\Lambda K}}{u-m_{N^*}^{\,2}}, \tag{11}$$

$$A_{\Sigma\Lambda,\Sigma^0}=\frac{eg_{\Sigma^0pK}}{u-m_2^{\,2}}+\frac{g_{\gamma KK^*}g^{E}_{K^*\Sigma p}(m_1+m_2)}{m(t-m_{K^*}^{\,2})}+\frac{g_{\gamma KK^*}g^{M}_{K^*\Sigma p}t}{m(m_1+m_2)(t-m_{K^*}^{\,2})}+\frac{g_{\gamma pN^*}g_{N^*\Sigma K}}{u-m_{N^*}^{\,2}}$$
$$+\frac{g_{\gamma\Delta N}g_{\Delta K\Sigma}}{3m_\pi^{\,2}}\left[t+\frac{m_1}{3m^*}(u-2m_2^{\,2}+m_1^{\,2}+2m_\mu^{\,2})+\frac{m_1m_2}{3m^{*2}}(u-m_2^{\,2}+m_\mu^{\,2})+\frac{m_1}{m^*}(m_2^{\,2}-m_1^{\,2})\right]\frac{1}{m^{*2}-u}. \tag{12}$$

We assume that the absorptive amplitudes are given exactly by Eqs. (11) and (12) for an energy range given by W^2 lying between the elastic threshold $W_{\rm th}^{\,2}=(m_p+m_K)^2$ and the inelastic threshold $W_{\rm in}^{\,2}=(m_p+m_K+m_\pi)^2$. The coupling constants are assumed to be given by their on-shell values. The absorptive parts of $F_2^{\Lambda,\Sigma^0,\Sigma\Lambda}(W^2)$ are obtained by integrating Eq. (3) with A given by Eqs. (11) and (12). The expressions for Im $F_2^{\Lambda,\Sigma^0,\Sigma\Lambda}$ are given in the Appendix.

The high-energy behaviors of the amplitudes are obtained by integrating Eq. (3) with the photoproduction amplitude A Reggeized by the replacements

$$\frac{1}{u-m_N^{\,2}}\to-\alpha'\Gamma(\tfrac{1}{2}-\alpha_N(u))\frac{1+\cos\pi(\alpha_N(u)-\frac{1}{2})}{2}\times s^{\alpha_N(u)-1/2}, \tag{13a}$$

$$\frac{1}{u-m_{N^*}^{\,2}}\to-\alpha'\Gamma(\tfrac{1}{2}-\alpha_{N^*}(u))\frac{1+\cos(\alpha_{N^*}(u)-\frac{1}{2})\pi}{2}\times s^{\alpha_{N^*}(u)-1/2}, \tag{13b}$$

$$\frac{1}{u-m_\Delta^{\,2}}\to\alpha'\Gamma(\tfrac{3}{2}-\alpha_\Delta(u))\frac{1-\cos\pi(\alpha_\Delta(u)-\frac{1}{2})}{2}\times s^{\alpha_\Delta(u)-3/2}, \tag{13c}$$

$$\frac{1}{t-m_{K^*}^{\,2}}\to-\alpha'\Gamma(1-\alpha_{K^*}(t))\frac{1-\cos\pi(\alpha_{K^*}(t))}{2}\times s^{\alpha_{K^*}(t)-1}. \tag{13d}$$

A plot of absorptive parts against $\ln(W^2)$ shows that the absorptive amplitudes vanish for large W^2 as $(W^2)^{-0.5}$ for Λ and as $(W^2)^{-0.35}$ for Σ^0 and $\Sigma\Lambda$ (see Fig. 3).

Extrapolation to the inelastic region is done by matching the perturbative Im $F_2^{\Lambda,\Sigma^0,\Sigma\Lambda}$ [Eqs. (A1), (A2), and (A3)] with Im $F_2(W^2)$ given by Eq. (7) with $y=0.5$ and 0.35 in the expression for $\Psi_R(z)$ [Eq. (10)]. Four terms of the series are found to be enough; they are given in Table II. Values of β, obtained by actual χ^2 plot, are 1.0, 1.6, and 1.6 for Λ, Σ^0, and $\Sigma\Lambda$, respectively (see Fig. 4). The results of fits below the inelastic threshold and the subsequent extrapolation are shown in

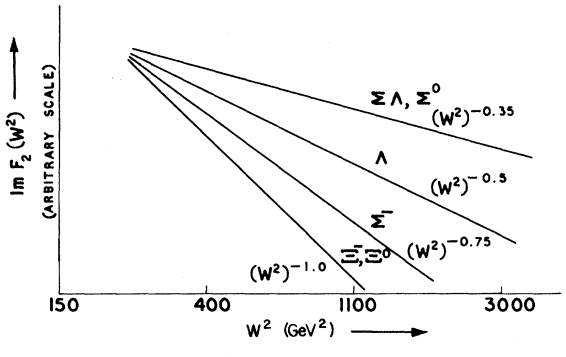

FIG. 3. Asymptotic behavior of absorptive amplitudes.

TABLE II. Values for the coefficients of the polynomial.

Baryon	Coefficient a_1	a_2	a_3	a_4
Λ	6.9748	0.8294	−0.1871	0.1002
Σ^0	−1.3523	0.1434	0.1104	−0.0281
$\Sigma\Lambda$	−3.2280	−0.4429	0.2537	−0.0358
Σ^- $\Lambda\pi$	1.7350	−0.1760	−0.1067	0.0034
$\Sigma\pi$	10.5080	−3.2043	−0.6982	−0.1885
Ξ^-	6.2347	−1.9661	−0.2951	−0.1882
Ξ^0	4.3226	−1.5170	−0.1692	−0.1612

TABLE III. Estimated contributions to the baryon anomalous magnetic moments (in nuclear magnetons) from Born and resonance terms. The intermediate states are indicated in parentheses below the values listed.

Baryon	Born term	Born term +t-channel resonance	Born term +t-channel resonance +u-channel resonance	Experimental values
Λ	−0.32	−0.498	−0.545	−0.67 ± 0.06
	(p)	(p +K^*)	[p +K^* +N^*(1460)]	
$\Sigma\Lambda$	0.202	0.34	0.97	
	(p)	(p +K^*)	[p +K^* +Δ(1236) +N^*(1460)]	
Σ^0	−0.069	0.037	0.4	
	(p)	(p +K^*)	[p +K^* +Δ(1236) +N^*(1460)]	
Σ^- $\Lambda\pi$	−0.245	−0.283		
	(Λ)	(Λ +ρ)	−0.493	−0.48 ± 0.37
$\Sigma\pi$	−0.052	−0.199	−0.21	
	(Σ)	(Σ +ρ)	(Σ +Y^* +ρ)	
Σ^+		$2\kappa_{\Sigma^0} - \kappa_{\Sigma^-} = 1.293$		1.59 ± 0.46
Ξ^-	−0.033	−0.297		−0.93 ± 0.75
	(Ξ)	(Ξ +ρ)		
Ξ^0	0.05	−0.214		
	(Ξ)	(Ξ +ρ)		

Figs. 5–7. Dispersion integrals are then evaluated and the results are shown in Table III.

IV. ANOMALOUS MAGNETIC MOMENTS OF $\Sigma^{+,-}$

The electromagnetic current behaves as $V_{\mu 3} + (1/\sqrt{3})V_{\mu 8}$ under SU(3) transformations. Assuming SU(2) invariance one can write

$$\langle \Sigma^+ | J_\mu | \Sigma^+ \rangle = \langle \Sigma | J^V_{\mu 3} | \Sigma \rangle + \langle \Sigma | J^S_\mu | \Sigma \rangle,$$

$$\langle \Sigma^0 | J_\mu | \Sigma^0 \rangle = \langle \Sigma | J^S_\mu | \Sigma \rangle,$$

and

$$\langle \Sigma^- | J_\mu | \Sigma^- \rangle = \langle \Sigma | J^S_\mu | \Sigma \rangle - \langle \Sigma | J^V_{\mu 3} | \Sigma \rangle,$$

where superscripts V and S refer to isovector and isoscalar parts of J_μ. Thus the anomalous magnetic moments of $\Sigma^{+,-,0}$ are related as follows[13]: $\kappa_{\Sigma^+} + \kappa_{\Sigma^-} = 2\kappa_{\Sigma^0}$. κ_{Σ^0} has already been calculated in the previous section. We encounter a difficulty in calculating the κ_{Σ^+} which will be explained later. So we choose to calculate κ_{Σ^-}.

The possible meson-baryon intermediate states are $\Sigma\pi$, $\Lambda\pi$, NK, and ΞK. The thresholds for

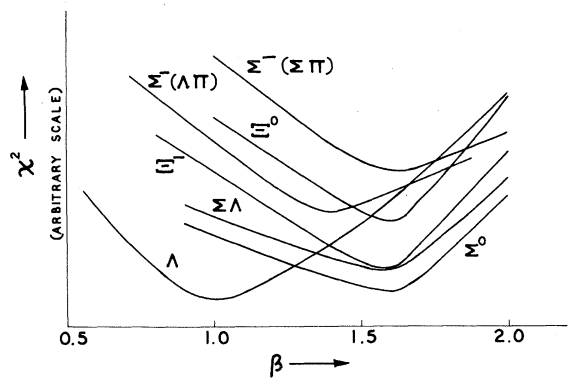

FIG. 4. χ^2 plot to determine phase factors.

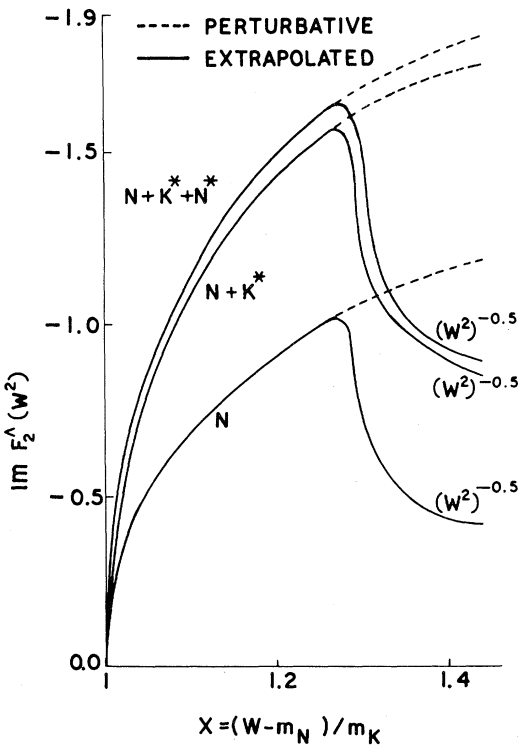

FIG. 5. Behavior of perturbative and extrapolated Im $F_2^\Lambda(W^2)$ with X, where $W^2 = (m_N + Xm_K)^2$.

NK and ΞK production lie much above the inelastic threshold, namely, the $\Lambda\pi\pi$ production threshold. We consider both the $\Sigma\pi$ and $\Lambda\pi$ intermediate states which lie below this inelastic threshold.

The photoproduction amplitudes for processes $\gamma+\Sigma^-\to\Lambda+\pi^-$ and $\gamma+\Sigma^-\to\Sigma^0+\pi^-$, $\Sigma^-+\pi^0$ with Born terms and the t- and u-channel resonances are given by

$$A^{\Sigma^-}_{\Lambda\pi}=\frac{-eg_{\Sigma\Lambda\pi}}{s-m_2^{\,2}}+\frac{g_{\gamma\pi\rho}g^{\Sigma}_{\rho\Sigma\Lambda}(m_1+m_2)}{m(t-m_\rho^{\,2})}+\frac{g_{\gamma\pi\rho}g^{M}_{\rho\Sigma\Lambda}t}{m(m_1+m_2)(t-m_\rho^{\,2})}, \tag{14}$$

$$A^{\Sigma^-}_{\Sigma\pi}=-eg_{\Sigma\Sigma\pi}\left(\frac{2}{s-m_2^{\,2}}+\frac{1}{u-m_2^{\,2}}\right)+\frac{g_{\gamma\rho\pi}g^{B}_{\rho\Sigma\Sigma}(m_1+m_2)}{m(t-m_\rho^{\,2})}+\frac{g_{\gamma\rho\pi}g^{M}_{\rho\Sigma\Sigma}t}{m(m_1+m_2)(t-m_\rho^{\,2})}$$
$$+\frac{g_{\gamma\Sigma Y^*}g_{Y^*\Sigma\pi}}{4m_\pi^{\,2}}\left[2t+\frac{2m_1}{3m^*}(u-2m_2^{\,2}+m_1^{\,2}+2m_\mu^{\,2})+\frac{2m_1m_2}{3m^{*\,2}}(u-m_2^{\,2}+m_\mu^{\,2})+\frac{2m_1}{m^*}(m_2^{\,2}-m_1^{\,2})\right]\frac{1}{m^{*2}-u}. \tag{15}$$

Integrating Eq. (3) with these A's one calculates the absorptive amplitudes Im $F^{\Sigma^-}_{2\Lambda\pi}$ and Im $F^{\Sigma^-}_{2\Sigma\pi}$; the expressions for these are given in the Appendix.

In the photoproduction amplitude for an incident Σ^+ baryon, there is the complication of a direct-channel Y^* resonance. This makes the amplitudes change sign, and the absorption changes drastically. Since matching procedure is best for smooth functions there will be uncertainties in the calculation of κ_{Σ^+} if this low-lying resonance is included. Hence we calculate κ_{Σ^-} and obtain κ_{Σ^+} from the relation $\kappa_{\Sigma^+}=2\kappa_{\Sigma^0}-\kappa_{\Sigma^-}$.

To obtain the high-energy behavior we integrate Eq. (3) with the pole terms of A Reggeized by the replacements

$$\frac{1}{u-m_\Lambda^{\,2}}\to-\alpha'\Gamma\left(\tfrac{1}{2}-\alpha_\Lambda(u)\right)\frac{1+\cos\pi(\alpha_\Lambda(u)-\frac{1}{2})}{2}\times s^{\alpha_\Lambda(u)-1/2}, \tag{16a}$$

$$\frac{1}{u-m_\Sigma^{\,2}}\to-\alpha'\Gamma\left(\tfrac{1}{2}-\alpha_\Sigma(u)\right)\frac{1+\cos\pi(\alpha_\Sigma(u)-\frac{1}{2})}{2}\times s^{\alpha_\Sigma(u)-1/2}, \tag{16b}$$

$$\frac{1}{u-m_{Y^*}^{\,2}}\to\alpha'\Gamma\left(\tfrac{3}{2}-\alpha_{Y^*}(u)\right)\frac{1-\cos\pi(\alpha_{Y^*}(u)-\frac{1}{2})}{2}\times s^{\alpha_{Y^*}(u)-3/2}, \tag{16c}$$

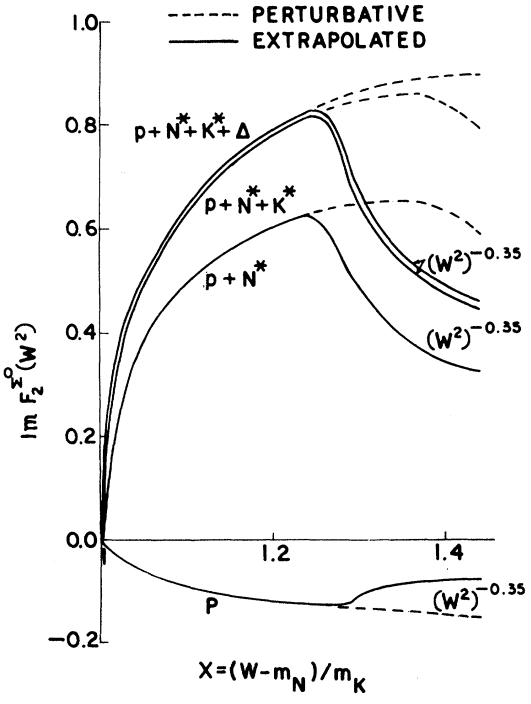

FIG. 6. Behavior of perturbative and extrapolated Im $F_2^{\Sigma^0}(W^2)$ with X, where $W^2=(m_N+Xm_K)^2$.

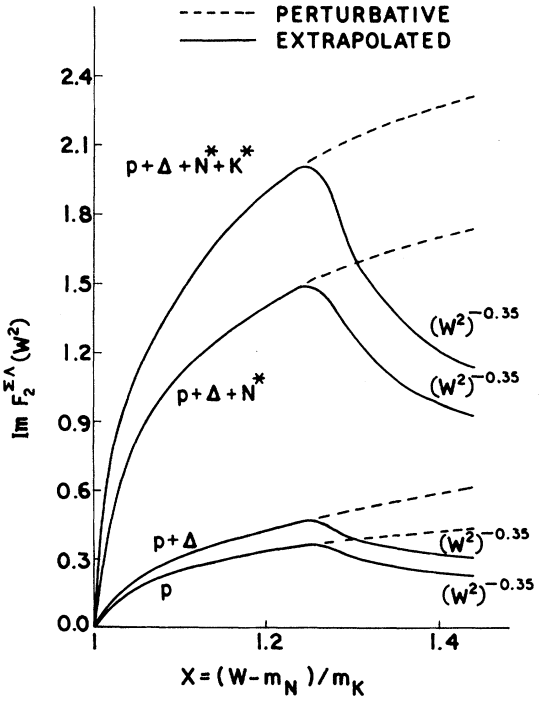

FIG. 7. Behavior of perturbative and extrapolated Im $F_2^{\Sigma\Lambda}(W^2)$ with X, where $W^2=(m_N+Xm_K)^2$.

$$\frac{1}{t-m_\rho{}^2} \to -\alpha'\Gamma(1-\alpha_\rho(t))\frac{1-\cos\pi\alpha_\rho(t)}{2} \times s^{\alpha_\rho(t)-1} \tag{16d}$$

and plot Im $F_2(W^2)$ against $\ln(W^2)$. The imaginary part is seen to vanish as $(W^2)^{-0.75}$ at high energies (see Fig. 3). This fixes the value of y in the expression for $\Psi_R(Z)$ [Eq. (10)].

We then match the polynomial [Eq. (7)] with Im $F^{\Sigma^-}_{2\Lambda\pi}$ and Im $F^{\Sigma^-}_{2\Sigma\pi}$ separately as given by Eqs. (A4) and (A5) in the energy intervals $W^2=(m_\Lambda+m_\pi)^2$ to $W^2=(m_\Lambda+2m_\pi)^2$ and $W^2=(m_\Sigma+m_\pi)^2$ to $W^2=(m_\Lambda+2m_\pi)^2$, respectively. Four terms of the series were found to be good enough for extrapolation (see Table II). The values of β obtained for minimum χ^2 fits are 1.4 and 1.6 (see Fig. 4). We have shown the fits in the specified energy ranges and the extrapolations beyond these ranges in Figs. 8(a) and 8(b). Dispersion integrals evaluated with these extrapolated absorptive amplitudes yield $\kappa_{\Sigma^-}=-0.493$. Using the SU(2) relation quoted above we get $\kappa_{\Sigma^+}=1.293$.

V. ANOMALOUS MAGNETIC MOMENTS OF $\Xi^{-,0}$

The two-body intermediate states which contribute to the absorptive amplitudes are $\Xi\pi$, ΣK, and ΛK for Ξ^- and $\Xi\pi$ and ΣK for Ξ^0. Of these we concentrate on $\Xi\pi$, which has the lowest threshold. For the photoproduction process $\gamma+\Xi^0\to\Xi^-+\pi^+$ the s channel is closed and A is given by the u-channel process $\gamma+\Xi^-\to\Xi^0+\pi^-$. For Ξ^-, the physical photoproduction amplitudes are given by the processes $\gamma+\Xi^-\to\Xi^-+\pi^0$, $\Xi^0+\pi^-$. Inclusion of the ρ resonance in the t channel [since SU(3) forbids electromagnetic coupling between Ξ^* and Ξ^-] gives

$$A_{\Xi^-}=-eg_{\Xi\Xi\pi}\left(\frac{3}{s-m_2{}^2}+\frac{1}{u-m_2{}^2}\right)+\frac{g_{\gamma\pi\rho}g^E_{\rho\Xi\Xi}(m_1+m_2)}{m(t-m_\rho{}^2)}+\frac{g_{\gamma\pi\rho}g^M_{\rho\Xi\Xi}t}{m(m_1+m_2)(t-m_\rho{}^2)}, \tag{17}$$

$$A_{\Xi^0}=-2eg_{\Xi\Xi\pi}\left(\frac{2}{s-m_2{}^2}+\frac{1}{u-m_2{}^2}\right)+\frac{g_{\gamma\pi\rho}g^E_{\rho\Xi\Xi}(m_1+m_2)}{m(t-m_\rho{}^2)}+\frac{g_{\gamma\pi\rho}g^M_{\rho\Xi\Xi}t}{m(m_1+m_2)(t-m_\rho{}^2)}. \tag{18}$$

The absorptive parts of $F_2(W^2)$ are obtained by integrating Eq. (3) with A's given by Eqs. (17) and

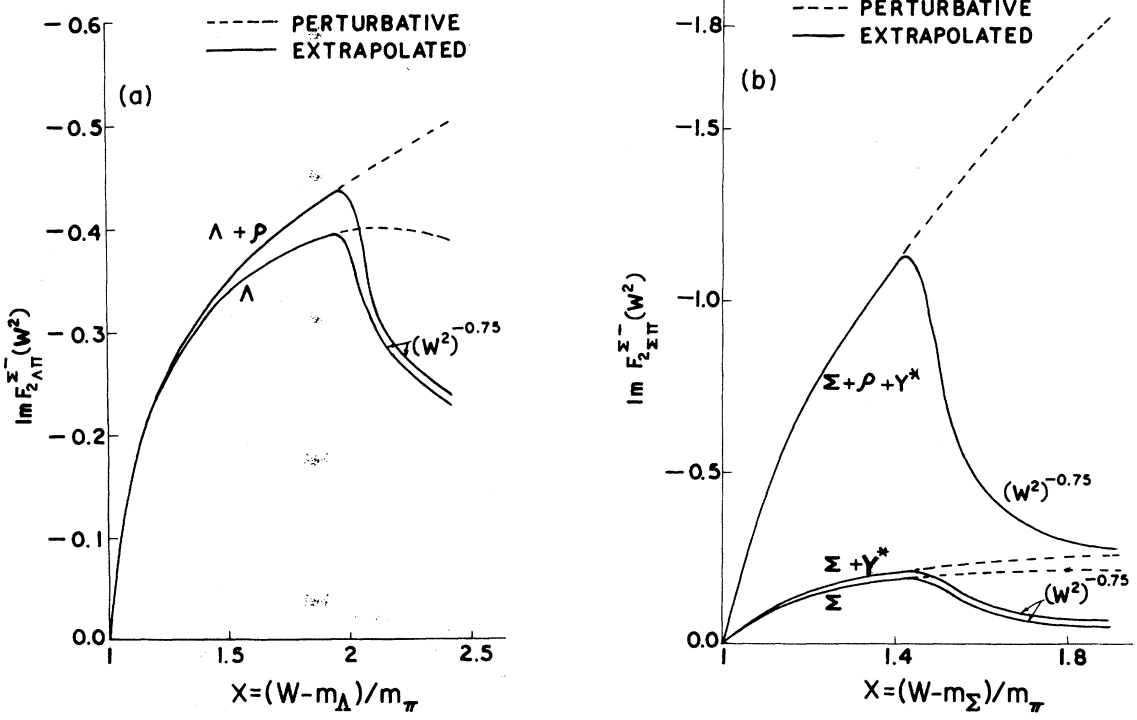

FIG. 8. (a) Behavior of perturbative and extrapolated Im $F^{\Sigma^-}_{2\Lambda\pi}(W^2)$ with X, where $W^2=(m_\Lambda+Xm_\pi)^2$. (b) Behavior of perturbative and extrapolated Im $F^{\Sigma^-}_{2\Sigma\pi}(W^2)$ with X, where $W^2=(m_\Sigma+Xm_\pi)^2$.

(18). The detailed expressions are given in the Appendix.

As in all previous cases we obtain the high-energy falloff by integrating Eq. (3) with the amplitudes modified by the usual substitutions for $1/(u-m_{\Xi}^2)$ and $1/(t-m_\rho^2)$. The graph of Im $F_2^{\Xi^0,\Xi^-}$ plotted against $\ln(W^2)$ shows that the absorptive amplitudes go to zero as $(W^2)^{-1.0}$ in the asymptotic energy limit (see Fig. 3). Extrapolation beyond the inelastic threshold corresponding to the production of a $\Xi\pi\pi$ state is done by matching Im $F_2^{\Xi^-}$ and Im $F_2^{\Xi^0}$ [Eqs. (A6) and (A7)] with only four terms of the series given by Eq. (7). The four coefficients are given in Table II. The β's, determined by minimum χ^2 fits, are found to be 1.6 for both cases (see Fig. 4). The fits between the elastic and inelastic thresholds and the extrapolations to higher energy regions are shown in Figs. 9 and 10. Evaluation of the dispersion integrals yields $\kappa_{\Xi^-} = -0.297$ and $\kappa_{\Xi^0} = -0.214$. The contributions due to the Born term and resonances are shown in Table III.

VI. DISCUSSIONS

The results obtained for baryon anomalous moments compare favorably with the experimental values, wherever these are available. This clearly endorses the view that the low-energy states along with the low-lying resonances contribute predominantly to the static properties of the elementary particles. As a check we have also calculated the additional contributions of various possible higher-mass meson-baryon intermediate states. The results, as shown in Table IV, are seen to be small and insignificant.

TABLE IV. Estimated contributions to the baryon anomalous magnetic moments (in nuclear magnetons) from possible higher-mass intermediate states.

Baryon	Intermediate baryon states: N	Λ	Σ	Ξ
p		0.052	negligible	
n			0.015	
Λ				0.002
Σ^0				0.021
Σ^-	−0.034			0.020
Ξ^-		−0.0026	negligible	
Ξ^0			−0.024	
$\Sigma\Lambda$				−0.019

Now we are in a position to discuss meaningfully the deviation of our results from those of pre-

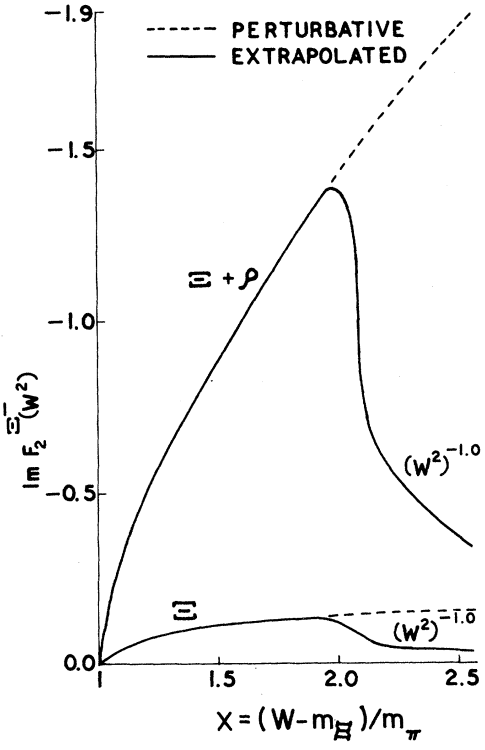

FIG. 9. Behavior of perturbative and extrapolated Im $F_2^{\Xi^-}(W^2)$ with X, where $W^2 = (m_\Xi + Xm_\pi)^2$.

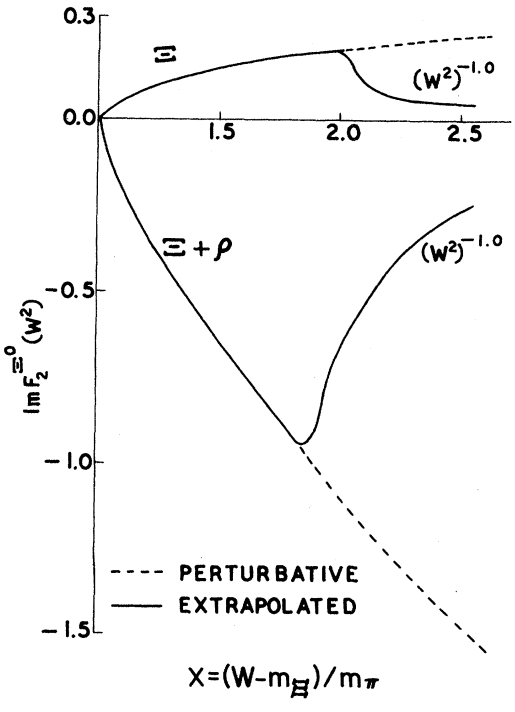

FIG. 10. Behavior of perturbative and extrapolated Im $F_2^{\Xi^0}(W^2)$ with X, where $W^2 = (m_\Xi + Xm_\pi)^2$.

vious workers. We recapitulate: Using threshold dominance, a cutoff, and SU(3) values for masses and coupling constants Pagels arrived at the results

$$\kappa_p = C(2g_{\pi N}^2 + g_{\Lambda K}^2 + g_{\Sigma K}^2),$$

$$\kappa_n = C(-2g_{\pi N}^2 + 2g_{\Sigma K}^2),\ \kappa_\Lambda = C(-g_{\Lambda K}^2 + h_{\Lambda K}^2),$$

$$\kappa_{\Sigma^-} = C(-g_{\Sigma\pi}^2 - 2g_{\Sigma K}^2 - g_{\Lambda\pi}^2),$$

$$\kappa_{\Sigma^0} = C(-g_{\Sigma K}^2 + h_{\Sigma K}^2),$$

$$\kappa_{\Sigma^+} = C(g_{\Sigma\pi}^2 + g_{\Lambda\pi}^2),$$

$$\kappa_{\Xi^-} = C(-h_{\Sigma K}^2 - h_{\Lambda\Sigma}^2 - 2g_{\Xi\pi}^2),$$

$$\kappa_{\Xi^0} = C(-2h_{\Xi K}^2 + 2g_{\Xi\pi}^2),$$

$$\kappa_\Sigma = C(-g_{\Sigma K}g_{\Lambda K} + h_{\Sigma K}h_{\Lambda K}),$$

where $C = \ln\Lambda/4\pi$ and Λ is the cutoff. The SU(3) prediction is recovered, but many moments turn out to be large. Only when the physical masses of the baryons and mesons are used and a rescattering term is fed in are the results in fair agreement with experiment (see Table I). However, in our analysis, we have only considered the states of lowest threshold, namely, πN for nucleons,[6] pK for Λ, Σ^0 and $\Sigma\Lambda, \Lambda\pi$, $\Sigma\pi$ for Σ^-, and $\Xi\pi$ for Ξ^- and Ξ^0. Since the absorptive amplitudes fall sharply beyond the inelastic threshold the contributions of high-mass two-body states such as ΛK, ΣK, ΞK, etc. are negligible and can be omitted. Resonances having masses around 1300 MeV contribute much more to the absorptive parts near threshold than do these high-mass two-body intermediate states. Hence substantial deviation from SU(3) is physically plausible, as is, indeed, seen by experiments. It may be noted that our analysis would lead to the SU(3) predictions in the limit of degenerate baryon masses and zero meson masses with a fixed Regge decrease for all the baryons and no resonance contributions to the relevant photoproduction amplitudes.

We finally note that our results are sensitive to the various coupling constants and the high-energy behaviors, which are the only unknown parameters of our analysis. In the present work we have taken the strengths and signs of various coupling constants as given by SU(3) with $D/(D+F) = 0.67$. The Regge behaviors, on the other hand, are obtained by actually plotting the absorptive amplitudes against W^2 for each baryon.

ACKNOWLEDGMENT

We are thankful to the personnel of the Computer Centre of Utkal University for all their help in computation.

APPENDIX

The absorptive amplitudes obtained by doing the integration of Eq. (3) with A having the general form

$$A = eg_{B_1B_2P}\left(\frac{1}{u-m_2^2} + \frac{1}{s-m_2^2}\right) + \frac{g_{\gamma PP^*}g^E_{P^*B_1B_2}(m_1+m_2)}{m(t-m_{P^*}^2)} + \frac{g_{\gamma PP^*}g^M_{P^*B_1B_2}t}{m(m_1+m_2)(t-m_{P^*}^2)} + \frac{g_{N^*B_2\gamma}\,g_{N^*B_1P}}{u-m_{N^*}^2}$$

$$+ \frac{g_{\gamma B^*B_2}g_{B^*B_1P}}{4m_\pi^2}\left[2t + \frac{2m_1}{3m^*}(u - 2m_2^2 + m_1^2 + 2m_\mu^2) + \frac{2m_1m_2}{3m^{*2}}(u - m_2^2 + m_\mu^2) + \frac{2m_1}{m^*}(m_2^2 - m_1^2)\right]\frac{1}{m^{*2}-u},$$

where B_1, B_1', B_2 are respectively the incoming, outgoing, and intermediate baryons, P, P^* are the meson and meson resonances of mass m_μ and m_{μ^*}, and B^* are decuplet resonances of mass m^*, can be written in the form

$$\text{Im } F_2(W^2) = F_u + F_s + F_{P^*} + F_{N^*} + F_{B^*},$$

where

$$F_u = \frac{g_{B_1'B_2P}g_{B_1B_2P}}{8\pi(W^2-m_1^2)}\left[m_1^2(x_+ - x_-) + m_1m_2\ln\frac{1-x_+}{1-x_-}\right],$$

$$F_s = \frac{g_{B_1'B_2P}g_{B_1B_2P}}{8\pi(W^2-m_1^2)}\left[(m_1m_2 - m_1^2)(x_+ - x_-) + \tfrac{1}{2}m_1^2(x_+^2 - x_-^2)\right],$$

$$F_{P^*} = \frac{m_1(m_1+m_2)}{8\pi me}\,\frac{g_{B_1'B_2P}\,g_{\gamma PP^*}\,g^E_{P^*B_1B_2}}{W^2-m_1^2}\left[\frac{(m_2-m_1)(W^2-m_1^2)+m_1(m_\mu^2-m_{\mu^*}^2)}{W^2-m_1^2}\ln\frac{m_\mu^2-m_{\mu^*}^2-(W^2-m_1^2)x_-}{m_\mu^2-m_{\mu^*}^2-(W^2-m_1^2)x_+}\right.$$

$$\left. - m_1(x_+ - x_-)\right]$$

$$+\frac{m_1 g_{B_1'B_2P}\, g_{\gamma PP^*}\, g^{M}_{P^*B_1B_2}}{8\pi e m(m_1+m_2)(W^2-m_1^2)}$$
$$\times\Big\{[(m_2-m_1)(W^2-m_1^2)-m_1 m_{\mu^*}{}^2](x_+-x_-)$$
$$+\frac{m_{\mu^*}{}^2[(m_2-m_1)(W^2-m_1^2)+m_1(m_\mu{}^2-m_{\mu^*}{}^2)]}{W^2-m_1^2}\ln\frac{m_\mu{}^2-m_{\mu^*}{}^2-(W^2-m_1^2)x_-}{m_\mu{}^2-m_{\mu^*}{}^2-(W^2-m_1^2)x_+}+m_1(W^2-m_1^2)\frac{x_+{}^2-x_-{}^2}{2}\Big\},$$

$$F_{N^*}=\frac{g_{B_1'B_2P}\, g_{N^*B_2\gamma}\, g_{N^*B_1P}}{8\pi e(W^2-m_1^2)}\left[m_1{}^2(x_+-x_-)+m_1 m_{N^*}\ln\frac{1-x_+}{1-x_-}\right],$$

$$F_{B^*}=\frac{g_{B_1'B_2P}\, g_{\gamma B_2B^*}\, g_{B^*B_1P}}{16\pi e m_\pi{}^2}$$
$$\times\Big\{\left[(m_1m_2-m_1^2)(x_+-x_-)+m_1\left(\frac{x_+{}^2-x_-{}^2}{2}\right)\right]$$
$$\times\left[\frac{X}{(W^2-m_1^2)(x_+-x_-)}\ln\frac{m^{*2}-m_2{}^2+(W^2-m_1^2)(1-x_-)}{m^{*2}-m_2{}^2+(W^2-m_1^2)(1-x_+)}+1-\frac{m_1}{3m^*}-\frac{m_1m_2}{3m^{*2}}\right]$$
$$-m_1{}^2(x_+{}^2-x_-{}^2)X\left[\frac{1}{(W^2-m_1^2)(x_+-x_-)}\right.$$
$$\left.-\frac{m^{*2}-m_2{}^2+(W^2-m_1^2)[1-\frac{1}{2}(x_++x_-)]}{(W^2-m_1^2)^2(x_+-x_-)^2}\ln\frac{m^{*2}-m_2{}^2+(W^2-m_1^2)(1-x_-)}{m^{*2}-m_2{}^2+(W^2-m_1^2)(1-x_+)}\right]\Big\},$$

with

$$x_\pm=\frac{W^2-m_2{}^2+m_\mu{}^2\pm\{[W^2-(m_2+m_\mu)^2][W^2-(m_2-m_\mu)^2]\}^{1/2}}{2W^2},$$

$$X=m_\mu{}^2-m^{*2}+m_1{}^2+m_2{}^2-W^2+\frac{m_1}{3m^*}(m^{*2}+m_1{}^2-2m_2{}^2+2m_\mu{}^2)+\frac{m_1m_2}{3m^{*2}}(m^{*2}-m_2{}^2+m_\mu{}^2)+\frac{m_1}{m^*}(m_2{}^2-m_1{}^2).$$

Now the absorptive amplitudes for the electromagnetic vertex of each baryon are given by

$$\text{Im}\, F_2^{\Lambda}(W^2)=F_u+F_{P^*}+F_{N^*}, \tag{A1}$$

with $B_1'=B_1=\Lambda$, $B_2=p$, $P=K$, $P^*=K^*$;

$$\text{Im}\, F_2^{\Sigma^0}(W^2)=F_u+F_{P^*}+F_{N^*}+\tfrac{2}{3}F_{B^*}, \tag{A2}$$

with $B_1'=B_1=\Sigma^0$, $B_2=p$, $P=K$, $P^*=K^*$, $B^*=\Delta(1236)$;

$$\text{Im}\, F_2^{\Sigma\Lambda}(W^2)=F_u+F_{P^*}+F_{N^*}+\tfrac{2}{3}F_{B^*}, \tag{A3}$$

with $B_1'=\Lambda$, $B_1=\Sigma^0$, $B_2=p$, $P=K$, $P^*=K^*$, $B^*=\Delta(1236)$;

$$\text{Im}\, F_{2\Lambda\pi}^{\Sigma^-}(W^2)=-F_s+F_{P^*}, \tag{A4}$$

with $B_1'=B_1=\Sigma^-$, $B_2=\Lambda$, $P=\pi$, $P^*=\rho$;

$$\text{Im}\, F_{2\Sigma\pi}^{\Sigma^-}(W^2)=-2F_s-F_u+F_{P^*}+F_{B^*}, \tag{A5}$$

with $B_1'=B_1=\Sigma^-$, $B_2=\Sigma$, $P=\pi$, $P^*=\rho$, $B^*=Y^*(1385)$;

$$\text{Im}\, F_2^{\Xi^-}(W^2)=-3F_s-F_u+F_{P^*}, \tag{A6}$$

with $B_1'=B_1=\Xi^-$, $B_2=\Xi$, $P=\pi$, $P^*=\rho$;

$$\text{Im}\, F_2^{\Xi^0}(W^2)=-2F_s-2F_u+F_{P^*}, \tag{A7}$$

with $B_1'=B_1=\Xi^0$, $B_2=\Xi$, $P=\pi$, $P^*=\rho$.

[1]Particle Data Group, Rev. Mod. Phys. 45, S1 (1973).
[2]S. Coleman and S. L. Glashow, Phys. Rev. Lett. 6, 423 (1961); S. Okubo, Phys. Lett. 4, 14 (1963).
[3]H. Katsumori, Prog. Theor. Phys. 18, 375 (1957).
[4]S. D. Drell and H. R. Pagels, Phys. Rev. 140, B397 (1965).
[5]H. Pagels, Phys. Rev. 140, B999 (1965).
[6]B. B. Deo and L. P. Singh, Phys. Rev. D 10, 308 (1974).
[7]A. M. Bincer, Phys. Rev. 118, 855 (1960).
[8]R. E. Cutkosky and B. B. Deo, Phys. Rev. Lett. 20, 1272 (1968); Phys. Rev. 174, 1859 (1968); S. Ciulli, Nuovo Cimento 61A, 787 (1969).
[9]G. F. Chew, M. L. Goldberger, F. E. Low, and Y. Nambu, Phys. Rev. 106, 345 (1957).
[10]N. M. Kroll and N. A. Ruderman, Phys. Rev. 93, 233 (1954).
[11]S. A. Adjei, P. A. Collins, B. J. Hartley, K. J. M. Moriarty, and P. W. Moore, Ann. Phys. (N.Y.) 75, 405 (1973).
[12]A. M. Boyarski, F. Bulos, W. Busza, R. Diebold, S. D. Ecklund, G. E. Fischer, J. R. Rees, and B. Richter, Phys. Rev. Lett. 20, 300 (1968); A. M. Boyarski, F. Bulos, W. Busza, R. Diebold, S. D. Ecklund, G. E. Fisher, Y. Murata, J. R. Rees, B. Richter, and W. S. C. Williams, *ibid.* 22, 1131 (1969).
[13]R. Marshak, S. Okubo, and E. C. G. Sudarshan, Phys. Rev. 106, 599 (1957).